

# Influence of solvation on the structure of highly charged nanoparticles in salt-free solutions

Alexandros Chremos<sup>1, a)</sup> and Jack F. Douglas<sup>1, b)</sup>

Materials Science and Engineering Division, National Institute of Standards and Technology, Gaithersburg, MD, 20899, USA

(Dated: 5 March 2019)

We investigate the influence of ion and nanoparticle solvation on the structure of an aqueous salt-free solution of highly charged nanoparticles. In particular, we perform molecular dynamics simulations of a minimal model of highly charged nanoparticles with an explicit solvent and counter-ions, where the relative affinity of the counter-ions and the nanoparticle for the solvent is tunable through the variation of the relative strength of the dispersion interactions of both the nanoparticle and counter-ions. We show that the competitive solvation of the counter-ions and nanoparticles leads to significant changes in the structure of the nanoparticle solution, which ranges from relatively uncorrelated conformations to self-assembled string- and sheet-like structures. Based on our coarse-grained model, we construct a morphology diagram identifying the different structures that emerge in our model with the variation of the solvent affinity for the charged species. The emergence of these different heterogeneous structures arising from the differential solvation of the charged species demonstrates the essential role of the solvent in the description of charged nanoparticle solutions, and provides guidance for the development of a more predictive theory of the thermodynamic and transport properties of these complex fluids.

## I. INTRODUCTION

Colloidal particles acquire an electric charge through surface dissociation of counter-ions when these are dispersed in water or other polar solvents. These electrostatic repulsions, modified to various degrees by the screening effects of surrounding counter-ions, stabilize the colloidal suspensions against aggregation induced by attractive van der Waals interactions. The range and strength of the inter-colloidal interactions are highly tunable since the size and charge of the colloids can be varied extensively, making colloidal dispersions an excellent model system to investigate fundamental issues relating to charges in condensed matter systems. It is widely appreciated that the structure of charged colloids in aqueous solutions is crucial in a wide variety of biological and technologically important systems, e.g., coatings/paints,<sup>73</sup> aerosols,<sup>74</sup> ceramics,<sup>75,76</sup> self-healing membranes,<sup>77</sup> and for particle separation or water purification processes.<sup>78</sup>

Our original understanding on the behavior of charged particles in solutions is based on the mean field model of Derjaguin-Landau-Verwey-Overbeek,<sup>79,80</sup> known as the DLVO theory. While the DLVO theory has been repeatedly modified, e.g., Lifschitz theory of attractive forces,<sup>81,82</sup> ion fluctuation forces,<sup>82,83</sup> charge regulation in the double layer,<sup>84</sup> the core of the theory has remained unchallenged for half a century.<sup>85,86</sup> We also mention recent modeling by Podgornik and coworkers,<sup>87</sup> which addresses the impact of *charge fluctuations* effects neglected by DLVO theory on the interaction of charged colloidal particles. This work builds

on earlier work by Kirkwood and Shumaker<sup>88,89</sup> modeling charged proteins indicates that charge fluctuations can lead to appreciable attractive interactions between charged colloidal particles that are missed by the standard DLVO theory. Although this seems to be a promising theoretical development, there is still a need, in our view, for a theory of how ion and nanoparticle solvation influence these charge fluctuations in order to have a predictive theory of charged particle solutions. The purpose of the present work is to provide insights into the solvation effects to aid in theoretical developments along this line.

Professors Ise and Hashimoto, and their colleagues, made pioneering experimental studies<sup>90-98</sup> of the emergence of heterogeneous structure formation in charged colloidal solutions, providing a strong impetus for much of the modern research in this field. Their work overlaps with a series of experimental studies since the mid-1980's that has challenged a cornerstone of DLVO theory, i.e., like charges always repel. Notable examples from these studies include the demonstration of like-charged planar surfaces attracting each other at sufficiently strong electrostatic coupling,<sup>99</sup> visible stable voids in colloidal fluids and crystals<sup>92-94</sup> and the deduced effective interaction potentials,<sup>100</sup> vapor-liquid and reentrant transitions,<sup>92</sup> localized ordered structures coexisting with disordered regions,<sup>101</sup> highly ordered inhomogeneous colloidal single crystals.<sup>102,103</sup> These experimental studies clearly imply that attractive forces may exist between like-charged colloids, in disagreement with the DLVO theory. The existence of such attractive interactions, first apparently noted by Langmuir,<sup>104</sup> has great significance for understanding the structure of highly charged particles formed in setting concrete,<sup>105-107</sup> in understanding the cohesion of soils<sup>108</sup> and in the binding of highly charged polyelectrolytes, such as duplex DNA,<sup>109,110</sup> F-actin,<sup>111</sup> and

---

a) Electronic mail: alexandros.chremos@nist.gov

b) Electronic mail: jack.douglas@nist.gov

virus particles to each other<sup>112</sup> and to soil particles.<sup>113</sup> At present, these and related phenomena are being intensively studied by various experimental techniques. Despite considerable theoretical and computational effort,<sup>114–117</sup> the origin of attractive electrostatic forces between spherical, like-charged colloidal particles in bulk solution has remained unresolved.

Conventional modeling of charged colloids in solution almost exclusively relies on the primitive model<sup>118–121</sup> of ionic solutions in which all charged species are treated explicitly as charged hard spheres and the solvent enters the model through its influence on the permittivity of the continuous medium surrounding the charged species. However, this natural extension of the Debye-Hückel theory<sup>122–124</sup> of ionic solutions does not address the solvation of ions or colloidal particle and typically the inclusion of an explicit solvent is avoided due to the added complexity and computational cost of including an explicit solvent in the analytic or computational treatment. Recent studies by the authors have demonstrated that the added complexity introduced by the explicit solvent in the model allows us to address many effects in aqueous solutions of charged species, including the origin of attractive interactions between charged polymer chains in salt-free solutions,<sup>125,126</sup> the thermodynamic and dynamic properties of ionic solutions,<sup>127,128</sup> and the conformational coupling between the polyelectrolyte chain and the diffuse ions surrounding it.<sup>129–131</sup> Solvation is part of the fundamental physics of electrostatic and colloid solutions and cannot be neglected.

In the present paper, we extend our model used in polyelectrolyte solutions<sup>129,130</sup> to describe highly charged nanoparticles (colloids of size on the order of nanometers) in salt-free solutions. Nanoparticles, unlike polyelectrolyte chains, do not change in shape, making them an ideal model to quantify the effects of solvation on the structures of highly charged nanoparticle solution. In particular, we find that the variation of the solvation interactions leads to a wide range of nanoparticle structures, which are not anticipated by mean field theories. We quantify these nanoparticle structures with the use of two correlation functions, i.e., the radial distribution function and static structure factor, and we organize our findings by constructing a morphology diagram that describes the various structures that emerge from or model with the variation of the strength of the solvation for the charged species.

Our paper is organized as follows. In Section II contains details of the model and simulation methods. Results of the structure of highly charged nanoparticles in solution are presented in Section III. Section IV concludes the paper.

## II. MODEL AND METHODOLOGY

Our system is composed of  $N_p$  nanoparticles suspended in explicit Lennard-Jones (LJ) solvent particles,

some of which are charged to represent counter-ions. All dissolved ions and solvent particles are assigned the same mass  $m$ , size  $\sigma$ , strength of interaction  $\varepsilon$ ; except as follows. Our nanoparticles are represented by a sphere, as the core particle, and  $N_{bb} = 64$  beads of diameter  $\sigma$  are bounded on its surface by stiff harmonic springs with the core particle, i.e.,  $V_H(r) = k(r - l_0)^2$ , where  $l_0 = 2\sigma$  is the equilibrium length of the spring, and  $k = 2000\varepsilon/\sigma^2$  is the spring constant. The surface beads cover completely the surface of the core particle; a schematic is presented in Fig. 1. The radius of the nanoparticle (core particle and surface beads) is approximately  $R \approx 2.2\sigma$ .

The size and energy parameters between  $i$  and  $j$  particles are set as  $\sigma_{ii} = \sigma_{jj} = \sigma_{ij} = \sigma$  and  $\varepsilon_{ii} = \varepsilon_{jj} = \varepsilon_{ij} = \varepsilon$ , except for: the interaction parameter between the solvent particles and the positively charged counter-ions  $\varepsilon_{cs}$  and the interaction parameter between the solvent particles and the nanoparticle beads  $\varepsilon_{ps}$ . Variation of the interaction energy parameters between the solvent and the charged particles reflects the strength of the solvent affinity<sup>127,128</sup> and the degree of chemical incompatibility.<sup>132</sup> For example,  $\varepsilon_{cs}/\varepsilon$  reflects the solvent affinity of water for the counter-ions and different values correspond to different types of monovalent ions, e.g. for caesium ( $\text{Cs}^+$ )  $\varepsilon_{cs}/\varepsilon = 0.83$ , for sodium ( $\text{Na}^+$ )  $\varepsilon_{cs}/\varepsilon = 1.25$ , and lithium ( $\text{Li}^+$ )  $\varepsilon_{cs}/\varepsilon = 1.6$ . The nanoparticles have a molecular mass of  $M_w = N_{bb} + 1$ , carry a  $-e$  charge per bounded bead on its surface, where  $e$  is the elementary charge, and thus the total nanoparticle charge is  $Z_p = -N_{bb} e$ .

All charged particles interact via the Coulomb potential (with a cut-off distance  $10\sigma$ ) and a relatively short range Lennard-Jones potential of strength  $\varepsilon$ , and the particle-particle mesh method is used.<sup>133</sup> Interactions between solvent, ions, and particles composing the surface of the nanoparticles are described by the cut-and-shifted Lennard-Jones potential with a cutoff distance  $r_c = 2.5\sigma$ :

$$V(r) = \begin{cases} 4\varepsilon \left[ \left(\frac{\sigma}{r}\right)^{12} - \left(\frac{\sigma}{r}\right)^6 - \left(\frac{\sigma}{r_c}\right)^{12} + \left(\frac{\sigma}{r_c}\right)^6 \right] & r \leq r_c \\ 0 & r > r_c \end{cases} \quad (1)$$

The core-surface bead interactions are modeled as a purely repulsive Weeks-Chandler-Andersen (WCA) potential<sup>134</sup> with modification taking into account the difference in the particle size,<sup>135</sup>

$$V_c(r) = \begin{cases} 4\varepsilon \left[ \left(\frac{\sigma}{r-\Delta}\right)^{12} - \left(\frac{\sigma}{r-\Delta}\right)^6 + 0.25 \right] & r \leq r_{\min} \\ 0 & r > r_{\min} \end{cases} \quad (2)$$

where  $r_{\min} = r_c + \Delta$  and  $\Delta = 1\sigma$  for the core-surface beads; there are no interactions between the cores and the ions or the solvent particles.

The system is composed of a total of  $N = 256\,000$  particles in a periodic cube of side  $L$  and volume  $V = L^3$ . The system includes  $N_p$  nanoparticles and

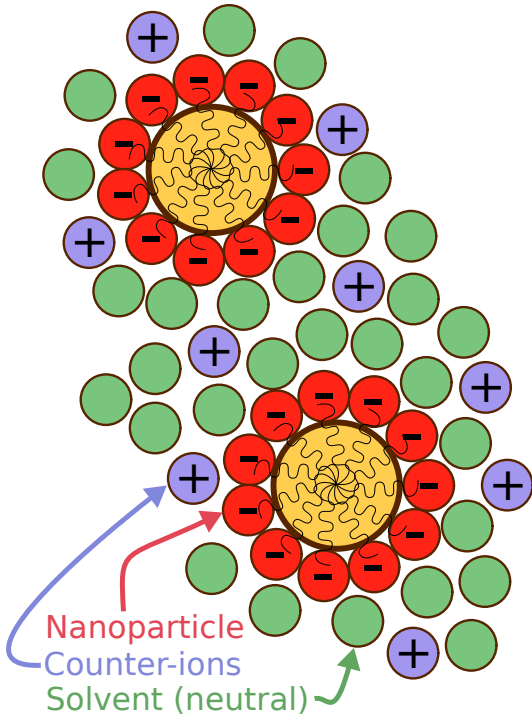


FIG. 1. Schematic of our charged nanoparticle solution model.

$N_+ = N_p |Z_p| e$  counter-ions so that all systems have neutral total charge. The number of solvent (neutral) particles is  $N_0 = N - N_+ - N_p M_w$ . We define the nanoparticle volume fraction as  $\varphi = N_p V_{\text{nano}} / V$ , where  $V_{\text{nano}} = 4\pi(d + \sigma)^3 / 24$ . For the purposes of our study we investigate systems that have  $\varphi \approx 0.004$ , corresponding to  $N_p = 100$ , unless stated otherwise. The Bjerrum length was set equal to  $l_B = e^2 / (\epsilon_s k_B T) = 2.4 \sigma$ , where  $T$  is the temperature,  $k_B$  is Boltzmann's constant, and  $\epsilon_s$  is the dielectric constant of the medium. The systems were equilibrated at constant pressure and constant temperature conditions, i.e., reduced temperature  $k_B T / \epsilon = 0.75$  and reduced pressure  $\langle P \rangle \sigma^3 / \epsilon \approx 0.02$ , and the production runs were performed at constant temperature constant volume, maintained by a Nosé-Hoover thermostat. Typical simulations equilibrate for  $4000 \tau$  and data is accumulated over a  $10000 \tau$  interval, where  $\tau = \sigma(m/\epsilon)^{1/2}$  is the MD time unit; the time step used was  $\Delta t / \tau = 0.005$ .

### III. RESULTS & DISCUSSION

We construct a morphology diagram of the various nanoparticle solution structures formed with the variation of the solvent affinity for the charged species; see Fig. 2a. Note that the nanoparticle volume fraction in the solution remains the same in all cases with  $\varphi \approx 0.004$  and there is no change in the basic mean field electrostatic quantities such as the Bjerrum length

and Debye screening length. It is evident from this diagram, as well as from simulation snapshots, that there are significant changes in the structure of the nanoparticles with the variation of the strength of solvation for the charged species, demonstrating that the solvation effects are crucial for the description of charged nanoparticles in solution. We briefly mention that the self-assembly of branched polymeric structures of ionic species has previously been observed to form similar branched particle dynamic structures in the context of modeling biomineralization,<sup>136</sup> a phenomenon that appears similar to the observations of the present work on charged nanoparticles.

To distinguish the various nanoparticle structures, we quantify the structure of highly charged nanoparticles in salt-free solutions with spatial correlations, such as the pair correlation function  $g(r)$  and its Fourier transform, the static structure factor,  $S(q)$ .<sup>137</sup> The radial distribution function between nanoparticles is defined as,

$$g(r) = \frac{\rho(r)}{\rho}, \quad (3)$$

where  $\rho$  is the total nanoparticle density and  $\rho(r)$  is the local density as function of distance,  $r$ , from a given nanoparticle. To understand the structural nature of nanoparticle assemblies at larger length scales, we use  $S(q)$ , which is defined for a collection of point particles as,

$$S(q) = \frac{1}{N_s} \left\langle \sum_{j=1}^{N_s} \sum_{k=1}^{N_s} \exp[-i\mathbf{q} \cdot (\mathbf{r}_j - \mathbf{r}_k)] \right\rangle, \quad (4)$$

where  $i = \sqrt{-1}$ ,  $q = |\mathbf{q}|$  is the wave number,  $\mathbf{r}_j$  is the position of particle  $j$ ,  $\langle \rangle$  denote the time average.

Now that we have defined the spatial correlations and before we proceed with the characterization of different morphologies, we briefly make a comparison of our model with the two cases. These two cases are to be compared with charged nanoparticle solution in an explicit solvent, where we first consider a solvent having no preferential solvation between the counter-ions and the nanoparticle. The neutral system corresponds to nanoparticles in an explicit solvent having  $\varphi \approx 0.004$  and no charges. As illustrated in Fig. 3, the neutral nanoparticles can approach each other at much shorter distances than the charged nanoparticles due to the lack of the repulsive electrostatic interactions, as expected. We also observe the tendency of uncharged nanoparticles to associate, mainly due to excluded volume based depletion interactions.<sup>138</sup> In the second case, we have charged nanoparticles and counter-ions but without any solvent particles. The interactions between the surface beads and counter-ions are changed to WCA to approximate the primitive model. Both explicit and implicit models result in qualitatively similar liquid-like nanoparticle solution structure, though in the latter the nanoparticles have less pronounced structural features; see Fig. 3. While this particular comparison between

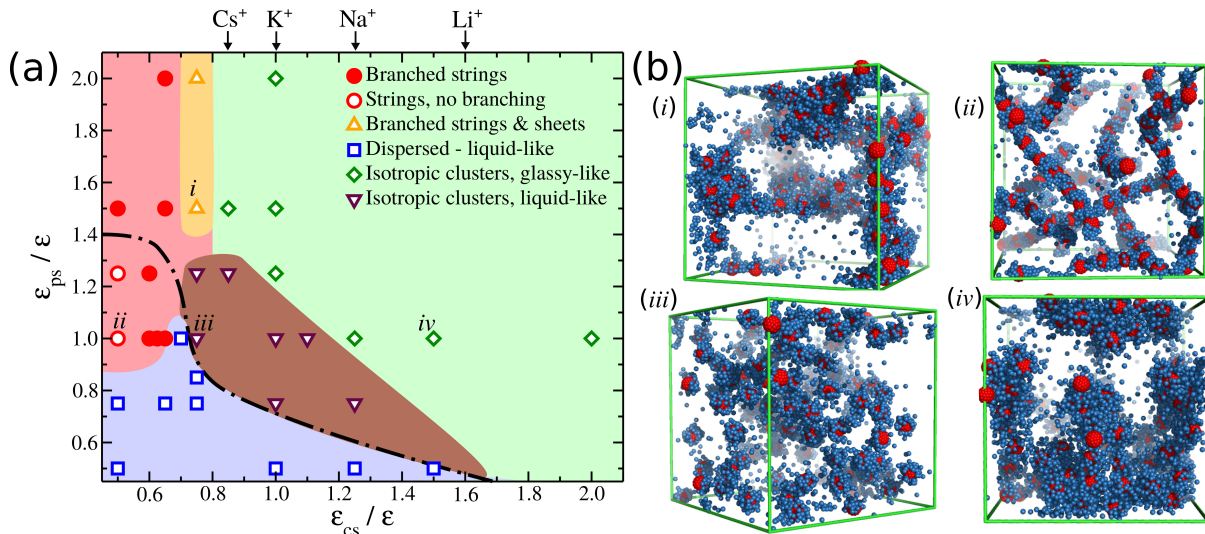


FIG. 2. (a) Morphology diagram of the nanoparticles at different the solvent affinities for the nanoparticles,  $\varepsilon_{ps}$ , and for the counter-ions,  $\varepsilon_{cs}$ . The dot-dashed line approximately describes the value of the static structure factor for the lowest wavevector value such that  $S(q_{\min}) = 1$ . Different salts (caesium, potassium, sodium, and lithium) are shown along the  $\varepsilon_{cs}$ -axis. (b) Typical snapshots of four different types of morphologies; the solvent (neutral) particles are rendered invisible for clarity. The roman labels point the location of the nanoparticle system in the morphology diagram.

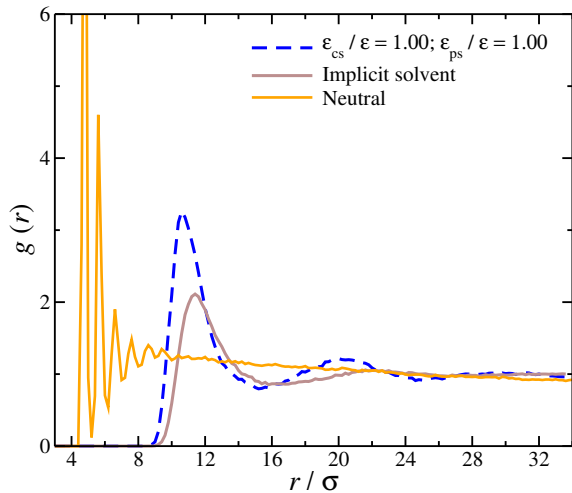


FIG. 3. Comparison of the radial distribution function  $g(r)$  of the nanoparticles with carrying charges in explicit solvent, neutral (no charge in explicit solvent), and carrying charges in implicit solvent.

explicit and implicit solvent models reveals small differences, we next show that the inclusion of a preferential solvent affinity for the charged species leads to significant deviations. This is the main topic of the present study and Fig. 3 provides a baseline comparison between the continuum theory and a charged particle solution in which there is solvation.

The deviations in  $g(r)$  and  $S(q)$  observed in our simulations reflect the formation of different structures and to distinguish them, we utilize two type of criteria.

Based on these criteria, five different type of structures (“morphologies”) are identified. These criteria are the following: (a) The form of  $g(r)$  provides information of the local structure, i.e., the packing of neighboring nanoparticles. In our case, we find three different forms namely, liquid-like, glass-like, and self-assembled string and sheet morphologies. For example, a glass-like structure is identified by a pronounced first peak in  $g(r)$  and the tendency of the second peak in  $g(r)$  to split. (b) The behavior of  $S(q)$  in low  $q$ , i.e., whether there is an excess scattering at low angles reflecting large density fluctuations or these density fluctuations are suppressed indicating a homogeneous system. For our purposes, we consider a system nearly homogeneous if  $S(q_{\min}) \leq 1$ , where  $q_{\min} = 2\pi/L$ .

When the solvent affinity for both the nanoparticles and the counter-ions is weak, then the nanoparticles are well dispersed in the solution, similar to the case of implicit solvent case, as illustrated in Fig. 3. This is evident from  $g(r)$ , where a liquid-like structure is found, but also in the structure factor  $S(q)$ , see Fig. 4. Additionally, the density fluctuations of nanoparticles, as indicated by the low  $q$ -regime in  $S(q)$ , are relatively suppressed, meaning that the nanoparticles are well dispersed in the solution. Note that the position of the first peak, which corresponds to the average distance between the nanoparticles, is located approximately at the same place as in the case of the implicit solvent. We identify nanoparticle systems that share these characteristics as “dispersed, liquid-like” systems.

An increase in the solvent affinity for the counter-ions  $\varepsilon_{cs}$ , while the solvent affinity for the nanoparticles remains weak  $\varepsilon_{ps}/\varepsilon \lesssim 1$ , progressively leads to a

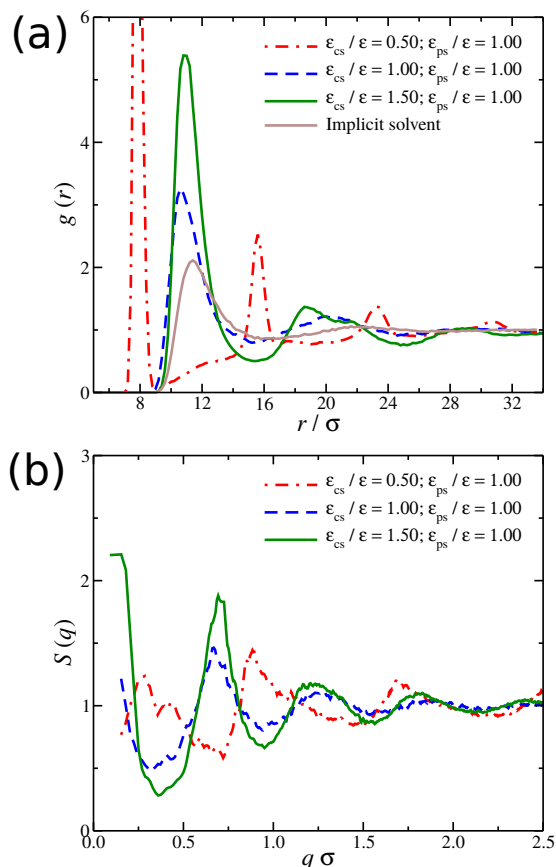


FIG. 4. Structural characterization of nanoparticle suspension for different solvent affinities with the counter-ions: (a) radial distribution function of the nanoparticles  $g(r)$  and (b) structure factor  $S(q)$  of the nanoparticles.

more pronounced liquid-like and then to glass-like characteristics; see Fig. 4a. At the same time, there is an increase in excess scattering exhibiting in  $S(q)$  at low  $q$ -values, suggesting that the system becomes heterogeneous; similar behavior has been observed in salt-free polyelectrolyte solutions.<sup>125</sup> Two different morphologies are identified. In the first morphology, the nanoparticles exhibit liquid-like structure, but start to become heterogeneously distributed, suggesting the formation of clusters. In the second regime, the nanoparticles form clusters and within these clusters the nanoparticles exhibit glass-like structure. The formation of clusters is more evident in the second regime as seen in Fig. 2b. The change in the structure of the nanoparticle solutions is induced by the solvent affinity for the counter-ions. This is a counter-intuitive result that mean field theory of ionic and colloidal solutions do not address. The ion and nanoparticle solvation affinity also apparently greatly influences the mobility of the solvated species, as discussed in electrolyte<sup>127,128</sup> and polyelectrolyte cases,<sup>125,131</sup> and by the extent its association with other charged species and eventual localization.<sup>131</sup> In other words, the localization of the counter-ions influ-

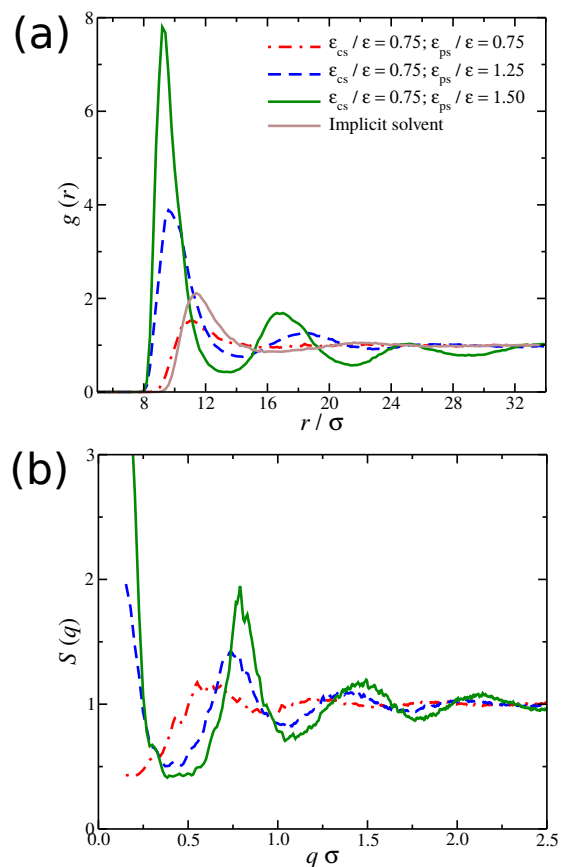


FIG. 5. Structural characterization of nanoparticle suspension for different solvent affinities with the nanoparticles: (a) radial distribution function of the nanoparticles  $g(r)$  and (b) structure factor of the nanoparticles  $S(q)$ .

ence the nanoparticle structure and transform it from a liquid-like to glass-like. These dynamical effects are accompanied by thermodynamic changes in the solution.

On the other hand, for low  $\varepsilon_{cs} \lesssim 0.65$ , the nanoparticles start to form string-like clusters; an illustration is presented in Fig 2b. As mentioned before, this phenomenon is remarkably similar in appearance to atomistic simulations and of ion association in water in the context of biomineralization.<sup>136,139</sup> The structural signature for the string formation is a pre-peak in  $g(r)$ , which progressively becomes more pronounced as  $\varepsilon_{cs}$  becomes smaller and eventually the peaks in  $g(r)$  occur at distances multiple of the location of the first peak, indicating the formation of a long relatively straight strings of nanoparticles equally spaced. Similar behavior was also found previously in solvent-free polymer grafted (uncharged) nanoparticles.<sup>140,141</sup> Away from the crossover point between liquid-like structure to string formation, the strings become long compared to the simulation box size that they percolate. When  $\varepsilon_{ps}/\varepsilon \approx 1$  and  $\varepsilon_{cs}/\varepsilon \lesssim 0.65$ , then we find that the strings have no branched points, Fig. 2. We are clearly observing a type of self-assembly process.<sup>139</sup>

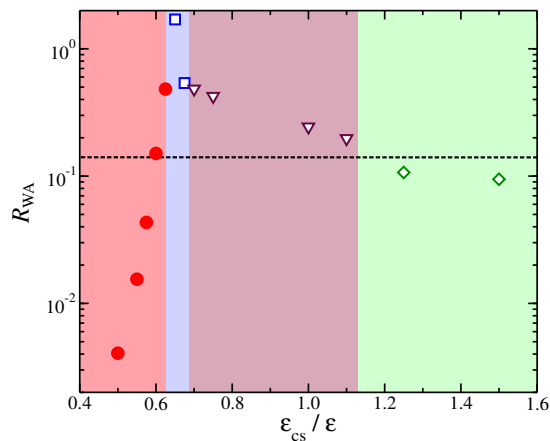


FIG. 6. Wendt-Abraham parameter,  $R_{WA}$ , as a function of the counter-ion solvent affinity  $\varepsilon_{cs}$  for nanoparticle solvent affinity  $\varepsilon_{ps}/\varepsilon = 1.0$ . The symbols and highlighted regions correspond to different morphologies as described in Fig. 2. The dashed line represents the threshold  $R_{WA} \approx 0.14$  for which it is often used to identify the glass transition temperature in atomic and colloidal systems.

An increase in the solvent affinity for the nanoparticles  $\varepsilon_{ps}$ , while the solvent affinity for the counter-ions is weak  $\varepsilon_{cs}/\varepsilon \lesssim 0.8$ , controls the number of branched points in the formation of string-like clusters. As the solvent affinity for the nanoparticles becomes stronger,  $\varepsilon_{cs}/\varepsilon \approx 0.75$  and  $\varepsilon_{ps}/\varepsilon > 1.25$ , the number of branched points in the string-like clusters increase and eventually we observe the sheet formation. The resulting  $g(r)$  and  $S(q)$  trends with nanoparticle solvation variation is presented in Fig. 5. Our results suggest that the sheet formation requires a delicate balance of solvation between the nanoparticles and counter-ions.

To better quantify the boundaries between the different morphologies, we use the Wendt-Abraham parameter<sup>142</sup>  $R_{WA} = g_{\min}/g_{\max}$ , where  $g_{\min}$  and  $g_{\max}$  are, respectively, the values of  $g(r)$  at its first minimum and its first maximum. This metric is often used to identify the glass transition temperature in atomic<sup>142</sup> and charged colloidal systems,<sup>143</sup> which occurs at approximately  $R_{WA} \approx 0.14$ . The trends in  $R_{WA}$  with variation of  $\varepsilon_{cs}$  for  $\varepsilon_{ps}/\varepsilon = 1.0$  is presented in Fig. 6. In each morphology regime  $R_{WA}$  exhibits a monotonic increase for small values of  $\varepsilon_{cs}$  and for  $\varepsilon_{cs}/\varepsilon \gtrsim 0.65$   $R_{WA}$  decreases with variation with  $\varepsilon_{cs}$ . At the boundaries between the different morphology regions,  $R_{WA}$  trends change suggesting a structural change in the nanoparticle solution. The value of  $R_{WA}$  at the crossover from the formation of clusters having a liquid-like clusters to glass-like structure occurring at  $\varepsilon_{cs}/\varepsilon \approx 1.1$ , is in good agreement with the identification of glass transition temperature often used in atomic and colloidal systems. Interestingly, for  $\varepsilon_{cs}/\varepsilon \approx 0.6$  the formation of self-assembled strings also exhibit values of  $R_{WA} \approx 0.14$ , suggesting that  $R_{WA}$  can be used to identify strongly bounded nanoparticles in anisotropic assemblies. Overall, the trends are consis-

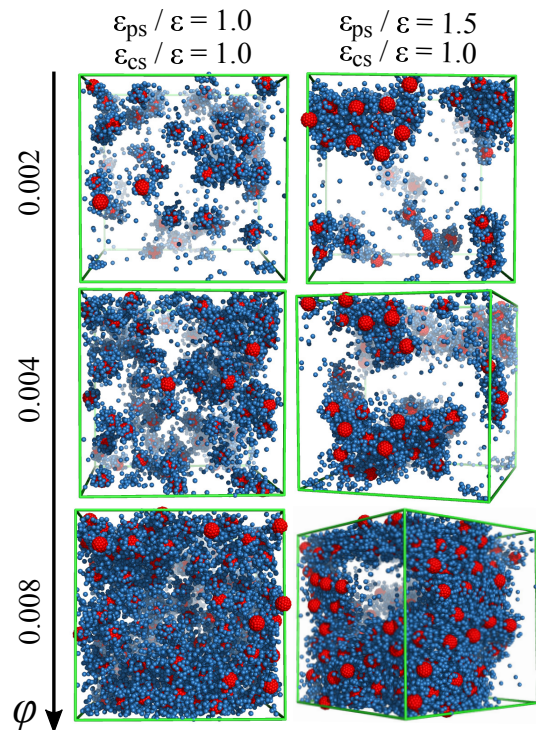


FIG. 7. Typical snapshots of nanoparticle solutions at different nanoparticle volume fractions,  $\varphi$ . Additionally, snapshots corresponding to two different solvent affinities are also presented. The solvent (neutral) particles are rendered invisible for clarity.

tent with the morphology diagram constructed in Fig. 2.

The formation of clusters of isolated nanoparticles in the form of compact clumps, linear and branched chains of particles and sheets is a phenomenon prevalent at low nanoparticle concentrations and new structures can be expected to arise at higher nanoparticle concentrations. At higher nanoparticle concentrations at which  $\varepsilon_{cs}/\varepsilon \gtrsim 1.1$  and/or  $\varepsilon_{ps}/\varepsilon \gtrsim 1.1$ , we observe the nanoparticle clusters to become bigger in size and eventually percolate, leading to the formation of ‘void’ regimes. The voids are occupied by the solvent, but are nearly devoid of charged particles. We show a representative particle configuration in this ‘concentrated’ charged nanoparticle regime in Fig. 7. Preliminary results show that the average size of the void regions, which are apparently stable, become smaller with increasing nanoparticle concentration. Similar void regimes, including their tunability with particle concentrations, were observed by Ise, Hashimoto, and coworkers in their studies<sup>93,94,96,97</sup> of sub-micro sized and highly charged colloidal particle suspensions. We have observed analogous voids in simulations of charged polyelectrolyte chains in which the solvent has high affinity for the counter-ions. In future work, we plan to study this ‘swiss cheese’ morphology of charged colloidal suspensions to determine the forces and dynamical effects that underlie cavity formation and structure. It is emphasized that the present

work focus at relatively low nanoparticle concentration regime.

#### IV. CONCLUSIONS

Professors Ise and Hashimoto, following in the footsteps of Langmuir<sup>104</sup> and Feynman,<sup>144</sup> made pioneering studies of highly charged particle suspensions with the aim of understanding the origin of the attractive interactions between highly charged particles and interfaces having the same sign, and the diverse practical and theoretical ramifications for this phenomenon. In this work, we have introduced a minimal model of highly charged nanoparticle solutions, where we can vary the relative strength of the dispersion interactions of the nanoparticle and counter-ions with the solvent, to gain insights into the structure of these solutions. We find that the solvation of the counter-ions and nanoparticles can lead to significant changes in the structure of the nanoparticles in the solution, reflecting the emergence of effective attractive interactions between the charged nanoparticles, just as we have seen before in salt-free polyelectrolyte solutions.<sup>125</sup> We have also found that these attractive interactions can lead to a more complex association processes than simple phase separation normally found for liquids exhibiting attractive short-ranged van der Waals interactions. Specifically, we find the formation of a wide range of nanoparticle complexes from anisotropic to isotropic supermolecular assemblies, where the net interactions originate from the ‘dressed’ nanoparticles and surrounding ions, a phenomenon anticipated by previous work<sup>139</sup> will arise from multi-pole interactions exhibited by associated particles and counter-ions. We anticipate an even greater wealth of structural behaviors to arise once we start exploring different nanoparticle concentrations, salt concentrations, nanoparticle sizes, nanoparticle surface charge density, etc. Overall, these results highlight the richness of structural behaviors exhibited by solvation in highly charged nanoparticles in salt-free solutions, demonstrating the essential role of the solvent in the description of the charged nanoparticle solutions, as well as providing a guideline for the development of a more predictive theory of the thermodynamic and transport properties of these complex fluids.

#### ACKNOWLEDGMENTS

We gratefully acknowledge the support of the NIST Director’s Office through the NIST Fellows’ postdoctoral grants program. Official contribution of the U.S. National Institute of Standards and Technology – not subject to copyright in the United States.

<sup>73</sup>T. F. Tadros, *Colloids in paints* (John Wiley & Sons, 2011).

<sup>74</sup>S. Lyonard, J. R. Bartlett, E. Sizgek, K. S. Finnie, T. Zemb, and J. L. Woolfrey, *Langmuir* **18**, 10386 (2002).

<sup>75</sup>I. Zhitomirsky, *Adv. Colloid Interface Sci.* **97**, 279 (2002).

- <sup>76</sup>M. A. Piechowiak, A. Videcoq, F. Rossignol, C. Pagnoux, C. Carrion, M. Cerbelaud, and R. Ferrando, *Langmuir* **26**, 12540 (2010).
- <sup>77</sup>N. Osterman, I. Poberaj, J. Dobnikar, D. Frenkel, and P. Z. D. Babic, *Phys. Rev. Lett.* **103**, 228301 (2009).
- <sup>78</sup>J. Buffle and G. G. Leppard, *Environ. Sci. Technol.* **29**, 2169 (1995).
- <sup>79</sup>B. V. Derjaguin and L. Landau, *Acta Physicochim (USSR)* **14**, 633 (1941).
- <sup>80</sup>E. J. Verwey and J. T. G. Overbeek, *Theory of the Stability of Lyophobic Colloids* (Elsevier, Amsterdam, 1948).
- <sup>81</sup>I. E. Dzyaloshinskii, E. M. Lifshitz, and L. P. Pitaevskii, *Adv. Phys.* **10**, 165 (1961).
- <sup>82</sup>J. Mahanty and B. W. Ninham, *Dispersion Forces* (Academic, London, 1976).
- <sup>83</sup>R. Kjellander, A. P. Lyubartsev, and S. Marčelja, *J. Chem. Phys.* **114**, 9565 (2001).
- <sup>84</sup>B. W. Ninham and V. A. Parsegian, *J. Theor. Biol.* **31**, 405 (1971).
- <sup>85</sup>B. V. R. Tata and S. S. Jena, *Solid State Commun.* **139**, 562 (2006).
- <sup>86</sup>M. Böstrom, D. R. M. Williams, and B. W. Ninham, *Phys. Rev. Lett.* **87**, 168103 (2001).
- <sup>87</sup>N. Adžić and R. Podgornik, *Phys. Rev. E* **91**, 022715 (2015).
- <sup>88</sup>J. G. Kirkwood and J. B. Shumaker, *Proc. Natl. Acad. Sci. U.S.A.* **38**, 855 (1952).
- <sup>89</sup>J. G. Kirkwood and J. B. Shumaker, *Proc. Natl. Acad. Sci. U.S.A.* **38**, 863 (1952).
- <sup>90</sup>N. Ise, *Angew. Chem. Int. Engl.* **25**, 323 (1986).
- <sup>91</sup>N. Ise, *Phys. Chem. Chem. Phys.* **12**, 10279 (2010).
- <sup>92</sup>N. Ise, K. Ito, H. Matsuoka, and H. Yoshida, in *Ordering and Phase Transitions in Charged Colloids*, edited by A. K. Arora and B. V. R. Tata (VCH Publishers, New York, 1996), chap. 5, p. 101.
- <sup>93</sup>K. Ito, H. Yoshida, and N. Ise, *Science* **263**, 66 (1994).
- <sup>94</sup>H. Yoshida, N. Ise, and T. Hashimoto, *J. Chem. Phys.* **103**, 10146 (1995).
- <sup>95</sup>J. Yamanaka, H. Yoshida, T. Koga, N. Ise, and T. Hashimoto, *Phys. Rev. Lett.* **80**, 5806 (1998).
- <sup>96</sup>H. Yoshida, J. Yamanaka, T. Koga, N. Ise, and T. Hashimoto, *Langmuir* **14**, 569 (1998).
- <sup>97</sup>H. Yoshida, J. Yamanaka, T. Koga, T. Koga, N. Ise, and T. Hashimoto, *Langmuir* **15**, 2684 (1999).
- <sup>98</sup>D. Yamaguchi, N. Miyamoto, T. Fujita, T. Nakato, S. Koizumi, N. Ohta, N. Yagi, and T. T. Hashimoto, *Phys. Rev. E* **85**, 011403 (2012).
- <sup>99</sup>L. Guldbbrand, B. Jönsson, H. Wennerström, and P. Linse, *J. Chem. Phys.* **80**, 2221 (1984).
- <sup>100</sup>D. G. Grier, *Nature* **393**, 621 (1998).
- <sup>101</sup>K. Ito, H. Nakamura, and N. Ise, *J. Chem. Phys.* **85**, 6143 (1986).
- <sup>102</sup>T. Konishi, N. Ise, H. Matsuoka, H. Yamaoka, I. Sogami, and T. Yoshiyama, *Phys. Rev. B* **51**, 3914 (1995).
- <sup>103</sup>T. Konishi and N. Ise, *J. Am. Chem. Soc.* **117**, 8422 (1995).
- <sup>104</sup>I. Langmuir, *J. Chem. Phys.* **6**, 873 (1938).
- <sup>105</sup>B. Jönsson, H. Wennerström, A. Nonat, and B. Cabane, *Langmuir* **20**, 6702 (2004).
- <sup>106</sup>B. Jönsson, A. Nonat, C. Labbez, B. Cabane, and H. Wennerström, *Langmuir* **21**, 9211 (2005).
- <sup>107</sup>C. Plassad, E. Lesniewska, I. Pochard, and A. Nonat, *Langmuir* **21**, 7263 (2005).
- <sup>108</sup>C. Labbez, B. Jönsson, I. Pochard, A. Nonat, and B. Cabane, *J. Phys. Chem. B* **110**, 9219 (2006).
- <sup>109</sup>V. A. Bloomfield, *Curr. Opin. Struct. Biol.* **6**, 334 (1996).
- <sup>110</sup>B. Luan and A. Aksimentiev, *J. Am. Chem. Soc.* **130**, 15754 (2008).
- <sup>111</sup>T. E. Angelini, H. Liang, W. Wriggers, and G. C. L. Wong, *Proc. Natl. Acad. Sci. U.S.A.* **100**, 8634 (2003).
- <sup>112</sup>A. P. Lyubartsev, J. X. Tang, P. A. Janmey, and L. Nordenkiöld, *Phys. Rev. Lett* **81**, 5465 (1998).
- <sup>113</sup>G. Bitton, *Water Research* **9**, 473 (1975).

- <sup>114</sup>L. Belloni, J. Chem. Phys. **88**, 5143 (1988).
- <sup>115</sup>H. Löwen, J. P. Hansen, and P. A. Madden, J. Chem. Phys. **98**, 3275 (1993).
- <sup>116</sup>M. Stevens, M. Falk, and M. Robbins, J. Chem. Phys. **104**, 5209 (1996).
- <sup>117</sup>B. Hribar and V. Vlachy, J. Phys. Chem. B **101**, 3457 (1997).
- <sup>118</sup>G. Stell, K. C. Wu, and B. Larsen, Phys. Rev. Lett. **37**, 1369 (1976).
- <sup>119</sup>E. Luijten, M. E. Fisher, and A. Z. Panagiotopoulos, Phys. Rev. Lett. **88**, 185701 (2002).
- <sup>120</sup>A. Z. Panagiotopoulos, J. Chem. Phys. **116**, 3007 (2002).
- <sup>121</sup>Y. C. Kim and M. E. Fisher, Phys. Rev. Lett. **92**, 185703 (2004).
- <sup>122</sup>P. Debye and E. Hückel, Phys. Z. **24**, 185 (1923).
- <sup>123</sup>D. A. McQuarrie, *Statistical Mechanics* (University Science Books, Sausalito, 2000).
- <sup>124</sup>H. Falkenhagen and W. Ebeling, Ionic Interactions **1**, 1 (2012).
- <sup>125</sup>A. Chremos and J. F. Douglas, J. Chem. Phys. **147**, 241103 (2017).
- <sup>126</sup>A. Chremos and J. F. Douglas, J. Chem. Phys. **149**, 163305 (2018).
- <sup>127</sup>M. Andreev, A. Chremos, J. de Pablo, and J. F. Douglas, J. Phys. Chem. B **121**, 8195 (2017).
- <sup>128</sup>M. Andreev, J. de Pablo, A. Chremos, and J. F. Douglas, J. Phys. Chem. B **122**, 4029 (2018).
- <sup>129</sup>A. Chremos and J. F. Douglas, Soft Matter **12**, 2932 (2016).
- <sup>130</sup>A. Chremos and J. F. Douglas, J. Chem. Phys. **144**, 164904 (2016).
- <sup>131</sup>A. Chremos and J. F. Douglas, Gels **4**, 20 (2018).
- <sup>132</sup>A. Chremos, A. Nikoubashman, and A. Z. Panagiotopoulos, J. Chem. Phys. **140**, 054909 (2014).
- <sup>133</sup>R. W. Hockney and J. W. Eastwood, *Computer Simulation Using Particles* (Taylor and Francis, New York, 1989).
- <sup>134</sup>J. D. Weeks, D. Chandler, and H. C. Andersen, J. Chem. Phys. **54**, 5237 (1971).
- <sup>135</sup>J. S. Smith, D. Bedrov, and G. D. Smith, Compos. Sci. Technol. **63**, 1599 (2003).
- <sup>136</sup>R. Demichelis, P. Raiteri, J. D. Gale, D. Quigley, and D. Gebauer, Nature **2**, 590 (2011).
- <sup>137</sup>J.-P. Hansen and I. R. McDonald, *Theory of simple liquids* (Academic Press, Cambridge, 2006).
- <sup>138</sup>H. N. Lekkerkerker and R. Tuinier, *Colloids and the depletion interaction* (Springer, 2011).
- <sup>139</sup>K. Van Workum and J. F. Douglas, Phys. Rev. E **73**, 031502 (2006).
- <sup>140</sup>A. Chremos and J. F. Douglas, Soft Matter **12**, 9527 (2016).
- <sup>141</sup>A. Chremos and J. F. Douglas, Annalen der Physik **529**, 1600342 (2017).
- <sup>142</sup>H. R. Wendt and F. F. Abraham, Phys. Rev. Lett. **41**, 1244 (1978).
- <sup>143</sup>B. V. R. Tata, P. S. Mohanty, and M. C. Valsakumar, Phys. Rev. Lett. **88**, 018302 (2002).
- <sup>144</sup>R. P. Feynman, R. B. Leighton, and M. Sands, *The Feynman Lecture on Physics* (Addison-Wesley, Reading, 1963), vol. I, chap. 2, pp. 3–4.
- <sup>73</sup>T. F. Tadros, *Colloids in paints* (John Wiley & Sons, 2011).
- <sup>74</sup>S. Lyonard, J. R. Bartlett, E. Sizgek, K. S. Finnie, T. Zemb, and J. L. Woolfrey, Langmuir **18**, 10386 (2002).
- <sup>75</sup>I. Zhitomirsky, Adv. Colloid Interface Sci. **97**, 279 (2002).
- <sup>76</sup>M. A. Piechowiak, A. Videcoq, F. Rossignol, C. Pagnoux, C. Carrion, M. Cerbelaud, and R. Ferrando, Langmuir **26**, 12540 (2010).
- <sup>77</sup>N. Osterman, I. Poberaj, J. Dobnikar, D. Frenkel, and P. Z. D. Babic, Phys. Rev. Lett. **103**, 228301 (2009).
- <sup>78</sup>J. Buffle and G. G. Leppard, Environ. Sci. Technol. **29**, 2169 (1995).
- <sup>79</sup>B. V. Derjaguin and L. Landau, Acta Physicochim (USSR) **14**, 633 (1941).
- <sup>80</sup>E. J. Verwey and J. T. G. Overbeek, *Theory of the Stability of Lyophobic Colloids* (Elsevier, Amsterdam, 1948).
- <sup>81</sup>I. E. Dzyaloshinskii, E. M. Lifshitz, and L. P. Pitaevskii, Adv. Phys. **10**, 165 (1961).
- <sup>82</sup>J. Mahanty and B. W. Ninham, *Dispersion Forces* (Academic, London, 1976).
- <sup>83</sup>R. Kjellander, A. P. Lyubartsev, and S. Marčelja, J. Chem. Phys. **114**, 9565 (2001).
- <sup>84</sup>B. W. Ninham and V. A. Parsegian, J. Theor. Biol. **31**, 405 (1971).
- <sup>85</sup>B. V. R. Tata and S. S. Jena, Solid State Commun. **139**, 562 (2006).
- <sup>86</sup>M. Böstrom, D. R. M. Williams, and B. W. Ninham, Phys. Rev. Lett. **87**, 168103 (2001).
- <sup>87</sup>N. Adžić and R. Podgornik, Phys. Rev. E **91**, 022715 (2015).
- <sup>88</sup>J. G. Kirkwood and J. B. Shumaker, Proc. Natl. Acad. Sci. U.S.A. **38**, 855 (1952).
- <sup>89</sup>J. G. Kirkwood and J. B. Shumaker, Proc. Natl. Acad. Sci. U.S.A. **38**, 863 (1952).
- <sup>90</sup>N. Ise, Angew. Chem. Int. Engl. **25**, 323 (1986).
- <sup>91</sup>N. Ise, Phys. Chem. Chem. Phys. **12**, 10279 (2010).
- <sup>92</sup>N. Ise, K. Ito, H. Matsuoka, and H. Yoshida, in *Ordering and Phase Transitions in Charged Colloids*, edited by A. K. Arora and B. V. R. Tata (VCH Publishers, New York, 1996), chap. 5, p. 101.
- <sup>93</sup>K. Ito, H. Yoshida, and N. Ise, Science **263**, 66 (1994).
- <sup>94</sup>H. Yoshida, N. Ise, and T. Hashimoto, J. Chem. Phys. **103**, 10146 (1995).
- <sup>95</sup>J. Yamanaka, H. Yoshida, T. Koga, N. Ise, and T. Hashimoto, Phys. Rev. Lett. **80**, 5806 (1998).
- <sup>96</sup>H. Yoshida, J. Yamanaka, T. Koga, N. Ise, and T. Hashimoto, Langmuir **14**, 569 (1998).
- <sup>97</sup>H. Yoshida, J. Yamanaka, T. Koga, T. Koga, N. Ise, and T. Hashimoto, Langmuir **15**, 2684 (1999).
- <sup>98</sup>D. Yamaguchi, N. Miyamoto, T. Fujita, T. Nakato, S. Koizumi, N. Ohta, N. Yagi, and T. T. Hashimoto, Phys. Rev. E **85**, 011403 (2012).
- <sup>99</sup>L. Guldbrand, B. Jönsson, H. Wennerström, and P. Linse, J. Chem. Phys. **80**, 2221 (1984).
- <sup>100</sup>D. G. Grier, Nature **393**, 621 (1998).
- <sup>101</sup>K. Ito, H. Nakamura, and N. Ise, J. Chem. Phys. **85**, 6143 (1986).
- <sup>102</sup>T. Konishi, N. Ise, H. Matsuoka, H. Yamaoka, I. Sogami, and T. Yoshiyama, Phys. Rev. B **51**, 3914 (1995).
- <sup>103</sup>T. Konishi and N. Ise, J. Am. Chem. Soc. **117**, 8422 (1995).
- <sup>104</sup>I. Langmuir, J. Chem. Phys. **6**, 873 (1938).
- <sup>105</sup>B. Jönsson, H. Wennerström, A. Nonat, and B. Cabane, Langmuir **20**, 6702 (2004).
- <sup>106</sup>B. Jönsson, A. Nonat, C. Labbez, B. Cabane, and H. Wennerström, Langmuir **21**, 9211 (2005).
- <sup>107</sup>C. Plassard, E. Lesniewska, I. Pochard, and A. Nonat, Langmuir **21**, 7263 (2005).
- <sup>108</sup>C. Labbez, B. Jönsson, I. Pochard, A. Nonat, and B. Cabane, J. Phys. Chem. B **110**, 9219 (2006).
- <sup>109</sup>V. A. Bloomfield, Curr. Opin. Struct. Biol. **6**, 334 (1996).
- <sup>110</sup>B. Luan and A. Aksimentiev, J. Am. Chem. Soc. **130**, 15754 (2008).
- <sup>111</sup>T. E. Angelini, H. Liang, W. Wriggers, and G. C. L. Wong, Proc. Natl. Acad. Sci. U.S.A. **100**, 8634 (2003).
- <sup>112</sup>A. P. Lyubartsev, J. X. Tang, P. A. Janmey, and L. Nordenskiöld, Phys. Rev. Lett. **81**, 5465 (1998).
- <sup>113</sup>G. Bitton, Water Research **9**, 473 (1975).
- <sup>114</sup>L. Belloni, J. Chem. Phys. **88**, 5143 (1988).
- <sup>115</sup>H. Löwen, J. P. Hansen, and P. A. Madden, J. Chem. Phys. **98**, 3275 (1993).
- <sup>116</sup>M. Stevens, M. Falk, and M. Robbins, J. Chem. Phys. **104**, 5209 (1996).
- <sup>117</sup>B. Hribar and V. Vlachy, J. Phys. Chem. B **101**, 3457 (1997).
- <sup>118</sup>G. Stell, K. C. Wu, and B. Larsen, Phys. Rev. Lett. **37**, 1369 (1976).
- <sup>119</sup>E. Luijten, M. E. Fisher, and A. Z. Panagiotopoulos, Phys. Rev. Lett. **88**, 185701 (2002).
- <sup>120</sup>A. Z. Panagiotopoulos, J. Chem. Phys. **116**, 3007 (2002).

- <sup>121</sup>Y. C. Kim and M. E. Fisher, *Phys. Rev. Lett.* **92**, 185703 (2004).
- <sup>122</sup>P. Debye and E. Hückel, *Phys. Z.* **24**, 185 (1923).
- <sup>123</sup>D. A. McQuarrie, *Statistical Mechanics* (University Science Books, Sausalito, 2000).
- <sup>124</sup>H. Falkenhagen and W. Ebeling, *Ionic Interactions* **1**, 1 (2012).
- <sup>125</sup>A. Chremos and J. F. Douglas, *J. Chem. Phys.* **147**, 241103 (2017).
- <sup>126</sup>A. Chremos and J. F. Douglas, *J. Chem. Phys.* **149**, 163305 (2018).
- <sup>127</sup>M. Andreev, A. Chremos, J. de Pablo, and J. F. Douglas, *J. Phys. Chem. B* **121**, 8195 (2017).
- <sup>128</sup>M. Andreev, J. de Pablo, A. Chremos, and J. F. Douglas, *J. Phys. Chem. B* **122**, 4029 (2018).
- <sup>129</sup>A. Chremos and J. F. Douglas, *Soft Matter* **12**, 2932 (2016).
- <sup>130</sup>A. Chremos and J. F. Douglas, *J. Chem. Phys.* **144**, 164904 (2016).
- <sup>131</sup>A. Chremos and J. F. Douglas, *Gels* **4**, 20 (2018).
- <sup>132</sup>A. Chremos, A. Nikoubashman, and A. Z. Panagiotopoulos, *J. Chem. Phys.* **140**, 054909 (2014).
- <sup>133</sup>R. W. Hockney and J. W. Eastwood, *Computer Simulation Using Particles* (Taylor and Francis, New York, 1989).
- <sup>134</sup>J. D. Weeks, D. Chandler, and H. C. Andersen, *J. Chem. Phys.* **54**, 5237 (1971).
- <sup>135</sup>J. S. Smith, D. Bedrov, and G. D. Smith, *Compos. Sci. Technol.* **63**, 1599 (2003).
- <sup>136</sup>R. Demichelis, P. Raiteri, J. D. Gale, D. Quigley, and D. Gebauer, *Nature* **2**, 590 (2011).
- <sup>137</sup>J.-P. Hansen and I. R. McDonald, *Theory of simple liquids* (Academic Press, Cambridge, 2006).
- <sup>138</sup>H. N. Lekkerkerker and R. Tuinier, *Colloids and the depletion interaction* (Springer, 2011).
- <sup>139</sup>K. Van Workum and J. F. Douglas, *Phys. Rev. E* **73**, 031502 (2006).
- <sup>140</sup>A. Chremos and J. F. Douglas, *Soft Matter* **12**, 9527 (2016).
- <sup>141</sup>A. Chremos and J. F. Douglas, *Annalen der Physik* **529**, 1600342 (2017).
- <sup>142</sup>H. R. Wendt and F. F. Abraham, *Phys. Rev. Lett.* **41**, 1244 (1978).
- <sup>143</sup>B. V. R. Tata, P. S. Mohanty, and M. C. Valsakumar, *Phys. Rev. Lett.* **88**, 018302 (2002).
- <sup>144</sup>R. P. Feynman, R. B. Leighton, and M. Sands, *The Feynman Lecture on Physics* (Addison-Wesley, Reading, 1963), vol. I, chap. 2, pp. 3–4.